

## Supporting information

to

### **Not just a fluidifying effect: omega-3 phospholipids induce formation of non-lamellar structures in biomembranes**

Augusta de Santis,<sup>a,b</sup> Giuseppe Vitiello,<sup>b,c</sup> Marie-Sousai Appavou,<sup>d</sup> Ernesto Scoppola,<sup>e</sup> Giovanna Fragneto,<sup>f</sup> Lester C. Barnsley,<sup>d,g</sup> Luke A. Clifton,<sup>h</sup> Maria Francesca Ottaviani,<sup>i</sup> Luigi Paduano,<sup>a,b</sup> Irene Russo Krauss,<sup>\*,a,b</sup> Gerardino D'Errico<sup>\*,a,b</sup>

<sup>a</sup> Department of Chemical Sciences, University of Naples Federico II, Naples, Italy.

<sup>b</sup> CSGI (Consorzio per lo Sviluppo dei Sistemi a Grande Interfase), Florence, Italy.

<sup>c</sup> Department of Chemical, Materials and Production Engineering, University of Naples Federico II, Naples, Italy.

<sup>d</sup> Jülich Centre for Neutron Science (JCNS) at Heinz Maier-Leibnitz Zentrum (MLZ), Forschungszentrum Jülich GmbH, Garching, Germany

<sup>e</sup> Max Planck Institut für Kolloid und Grenzflächenforschung, Potsdam, Germany

<sup>f</sup> Institut Laue-Langevin (ILL) Grenoble, France

<sup>g</sup> Current address Australian Synchrotron, ANSTO, Clayton, Australia

<sup>h</sup> ISIS Facility, Science and Technology Facilities Council, Rutherford Appleton Laboratory, Harwell Oxford, Didcot OX11 0QX, United Kingdom

<sup>i</sup> Department of Pure and Applied Sciences, University of Urbino, Urbino, Italy

\* To whom correspondence should be addressed.

Irene Russo Krauss, Tel: +39 081674227; Email: [irene.russokrauss@unina.it](mailto:irene.russokrauss@unina.it),

Gerardino D'Errico, Tel: +39 081674245; Email: [gderrico@unina.it](mailto:gderrico@unina.it)

**Table S1** Scattering Length Densities (*SLDs*) and Molecular Volumes (*V*) used as input values for the Neutron Reflectivity fitting procedure.

<b>Molecule</b>	<b>Chemical Formula</b>	<b><i>SLD</i></b> <b>[10<sup>-6</sup> Å<sup>-2</sup>]</b>	<b><i>V</i></b> <b>[Å<sup>3</sup>]</b>
<b>Heavy Water</b>	D <sub>2</sub> O	6.3752	30.0428
<b>Light Water</b>	H <sub>2</sub> O	-0.5594	29.9757
<b>POPC (Tail)</b>	C <sub>32</sub> H <sub>64</sub>	-0.2899	919.614
<b>POPC (Headgroup)</b>	C <sub>10</sub> H <sub>18</sub> PO <sub>8</sub> N	1.8652	322.100
<b>22:6-22:6PC (Tail)</b>	C <sub>42</sub> H <sub>62</sub>	0.6543	722.940
<b>22:6-22:6PC (Headgroup)</b>	C <sub>10</sub> H <sub>18</sub> PO <sub>8</sub> N	1.8652	322.100
<b>Silicon</b>	Si	2.0754	20.000
<b>Silicon Oxide</b>	SiO <sub>2</sub>	3.2698	48.200

**Table S2** Correlation time  $\tau$ , order parameter  $S$  and coupling constant  $\langle A \rangle$  for 5- and 14-PCSL as derived from EPR spectra simulation. Errors are within 1%.

$x_{22:6-22:6PC}$	$\tau$ (ns)		$S$		$\langle A \rangle$ (G)	
	5-PCSL	14-PCSL	5-PCSL	14-PCSL	5-PCSL	14-PCSL
<b>0</b>	8.4	1.39	0.42	0.15	14.5	14.17
<b>0.2</b>	7.44	1.22	0.42	0.15	14.43	14.16
<b>0.4</b>	7.34	1.13	0.418	0.15	14.43	14.15
<b>0.5</b>	7.25	0.75	0.415	0.145	14.43	14.41
<b>0.6</b>	6.23	0.38	0.4	0.14	14.47	14.55
<b>0.8</b>	5.56	0.37	0.403	0.13	14.48	14.55
<b>1.0</b>	5.45	0.21	0.403	0.105	14.49	14.67

**Table S3** Correlation time  $\tau$ , order parameter  $S$  and coupling constant  $\langle A \rangle$  as derived from EPR spectra simulation for different spin labels and two different POPC/22:6-22:6PC compositions. Errors are within 1%.

$x_{22:6-22:6PC}$	$\tau$ (ns)		$S$		$\langle A \rangle$ (G)	
	0.2	0.8	0.2	0.8	0.2	0.8
<b>5-PCSL</b>	7.44	5.56	0.42	0.403	14.43	14.49
<b>7-PCSL</b>	4.2	3.1	0.41	0.39	14.43	14.3
<b>10-PCSL</b>	2.65	1.7	0.33	0.29	14.23	14.23
<b>14-PCSL</b>	1.22	0.37	0.15	0.13	14.16	14.55

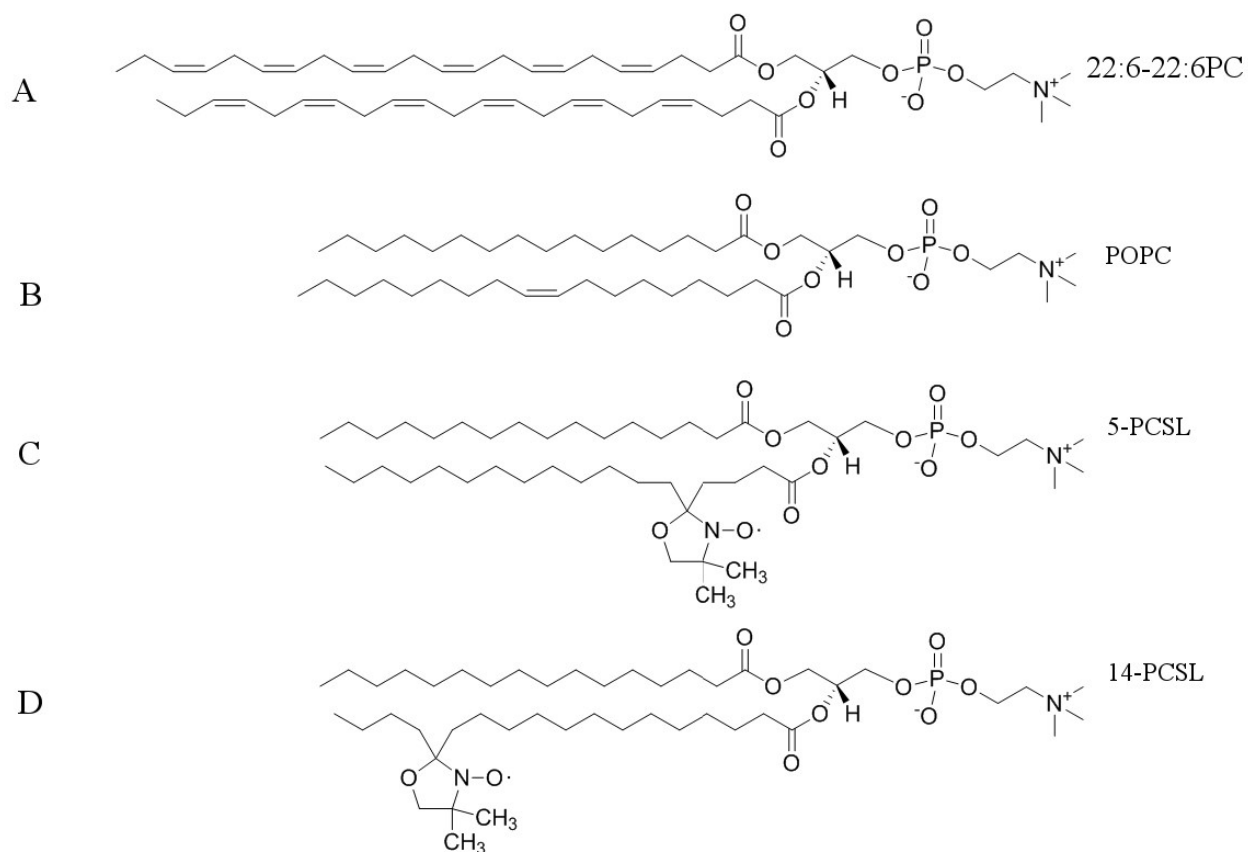


**Fig. S1** Chemical structure of the phospholipid employed in the study: 1,2-didocosahexaenoyl-*sn*-glycero-3-phosphocholine (22:6-22:6PC) (A), 1-palmitoyl-2-oleoyl-*sn*-glycero-3-phosphocholine (POPC) (B), 5-PCSL (C) and 14-PCSL (D).

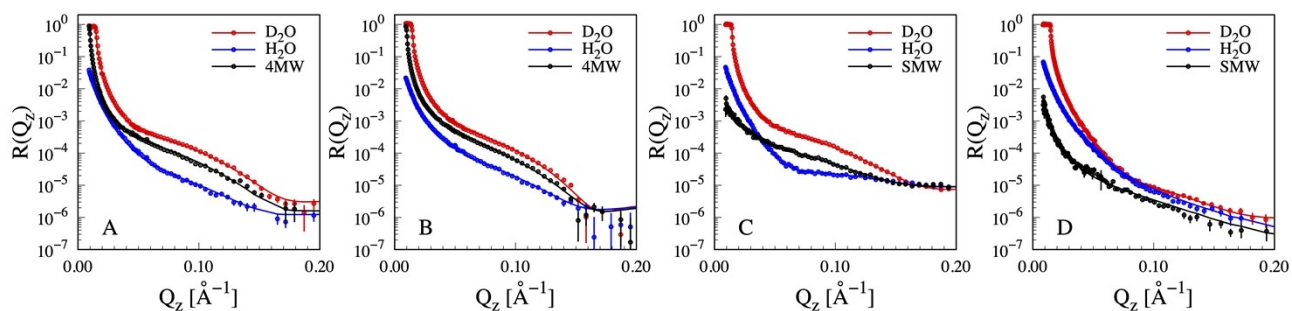


**Fig. S2** Experimental data and best fitting curves in D<sub>2</sub>O (red), H<sub>2</sub>O (blue) and either 4MW (black in panel A and B) or SMW (black in panel C and D) for lipid systems: A) POPC, B) POPC/22:6-22:6PC  $x_{22:6-22:6PC} = 0.2$ , C) POPC/22:6-22:6PC  $x_{22:6-22:6PC} = 0.4$ , D) POPC/22:6-22:6PC  $x_{22:6-22:6PC} = 0.8$  respectively.

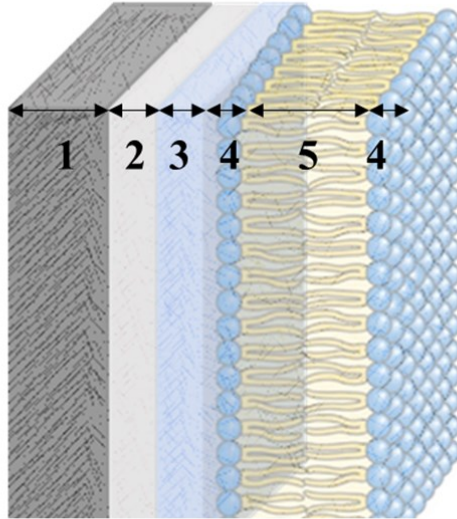


**Fig. S3** Schematic representation of the model used for fitting of NR profiles with all chemical components explicitly shown: 1) Si block; 2) SiO<sub>2</sub> layer; 3) water, 4) headgroups, 5) tails of the lipids forming the bilayer.

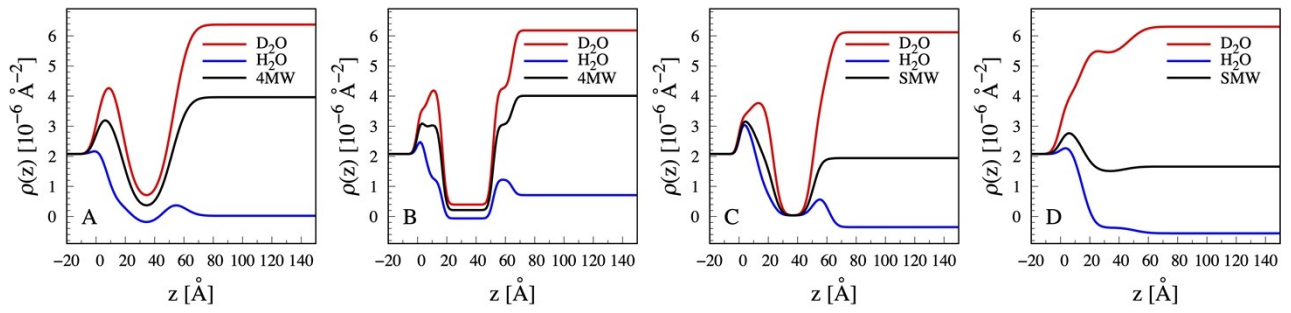


**Fig. S4** SLD profiles corresponding to best fit of Neutron Reflectivity data in D<sub>2</sub>O (red), H<sub>2</sub>O (blue) and either 4MW (black in panel A and B) or SMW (black in panel C and D) for lipid systems: A) POPC, B) POPC/22:6-22:6PC  $x_{22:6-22:6PC} = 0.2$ , C) POPC/22:6-22:6PC  $x_{22:6-22:6PC} = 0.4$ , D) POPC/22:6-22:6PC  $x_{22:6-22:6PC} = 0.8$ , respectively.



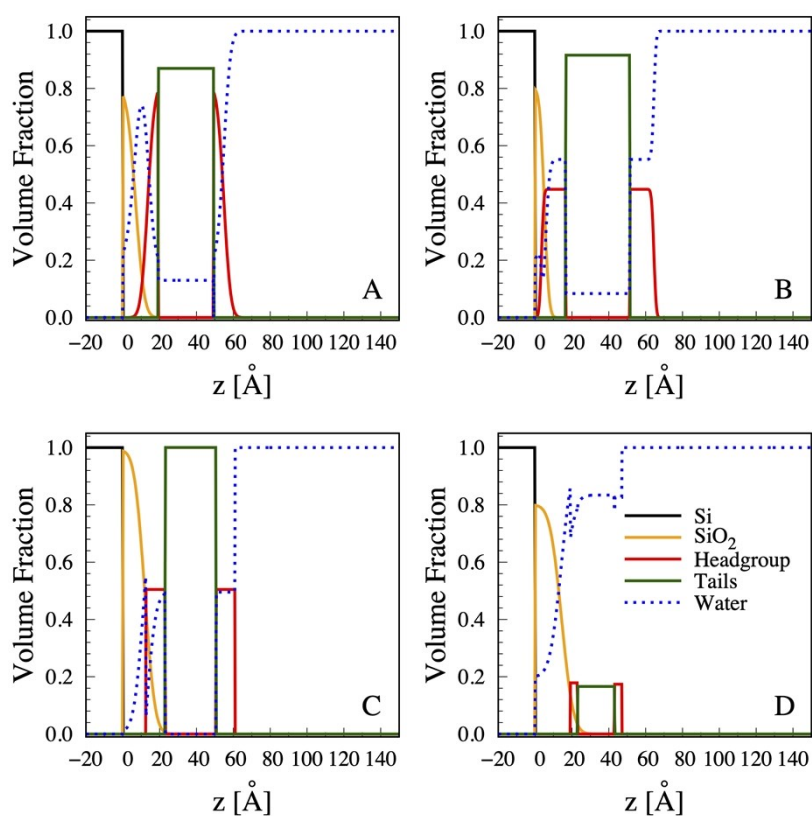
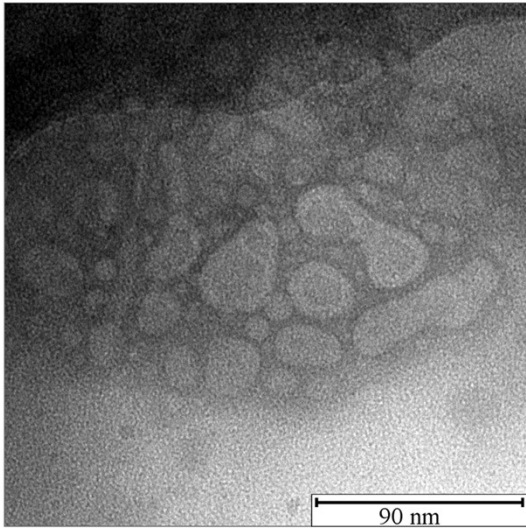
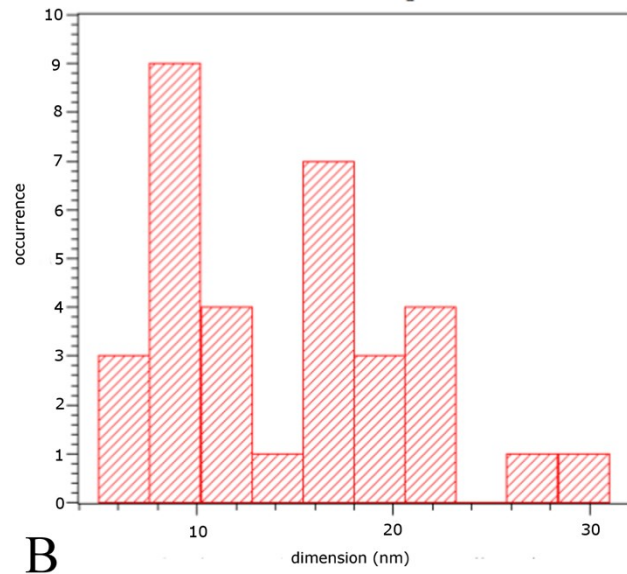


**Fig. S5** Deconvoluted volume fraction distribution profiles for Silicon (black), SiO<sub>2</sub> (orange), lipid headgroup (red), lipid tails (green) and water (dashed blue line) for lipid systems: A) POPC, B) POPC/22:6-22:6PC  $x_{22:6-22:6PC} = 0.2$ , C) POPC/22:6-22:6PC  $x_{22:6-22:6PC} = 0.4$  and D) POPC/22:6-22:6PC  $x_{22:6-22:6PC} = 0.8$ , respectively.



A



B

**Fig. S6** Cryo-TEM micrograph of POPC/22:6-22:6PC  $x_{22:6-22:6PC} = 0.8$  (A) and particle diameter distribution (B).

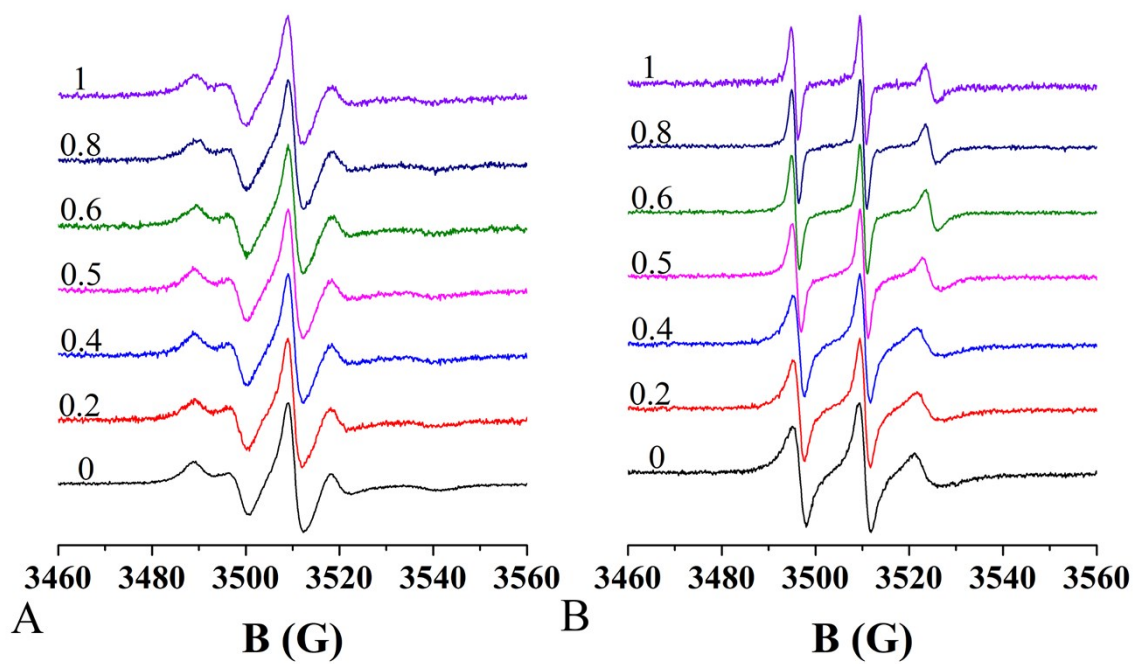


**Fig. S7** EPR spectra of 5-PCSL (A) and 14-PCSL (B), in POPC/22:6-22:6PC systems with  $X_{22:6-22:6PC}$  ranging from 0 to 1.

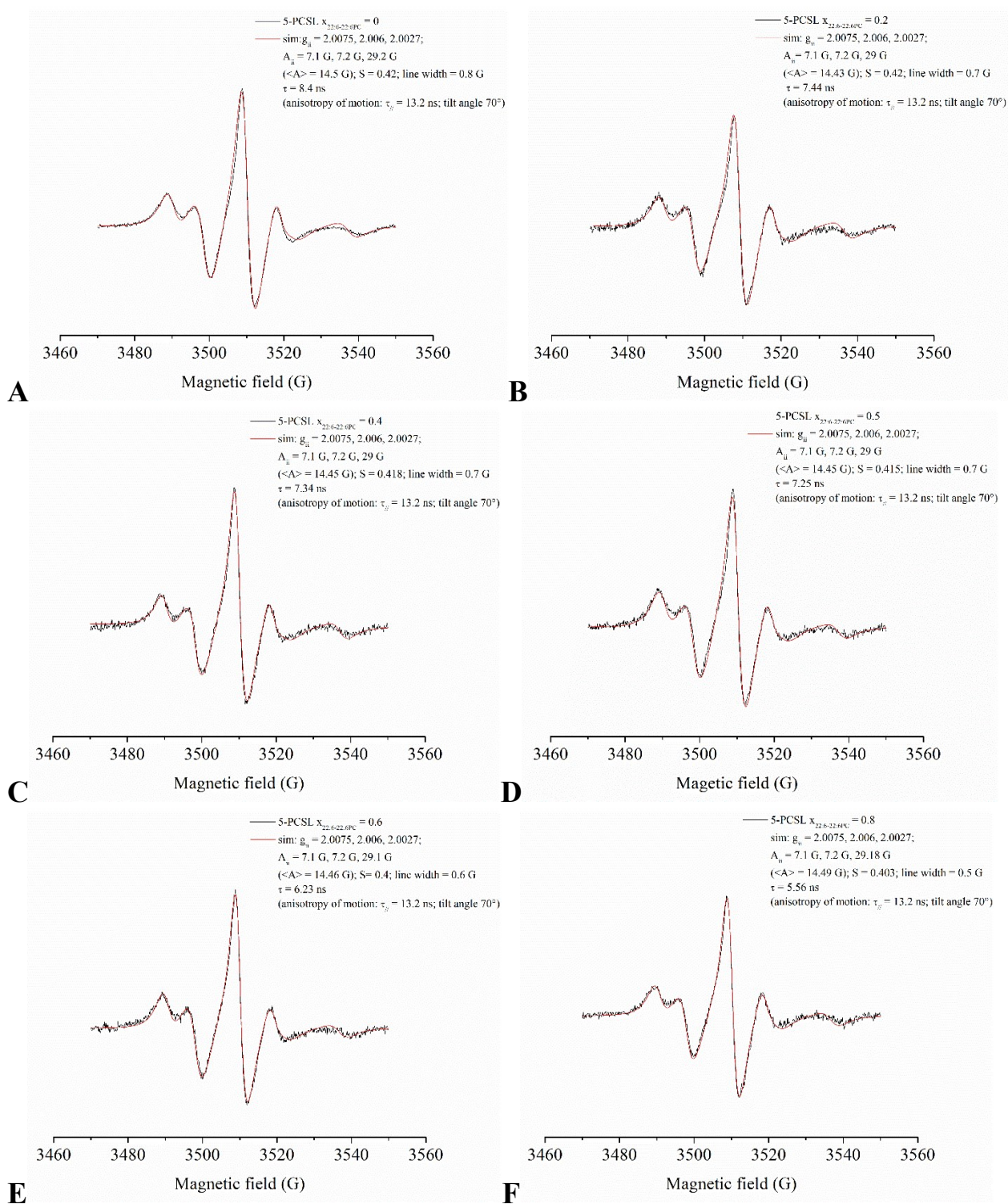


**Fig. S8** Comparison between simulated (red) and experimental (black) EPR spectra of 5-PCSL in POPC/22:6-22:6PC systems with  $x_{22:6-22:6PC}$  ranging from 0 to 0.8.

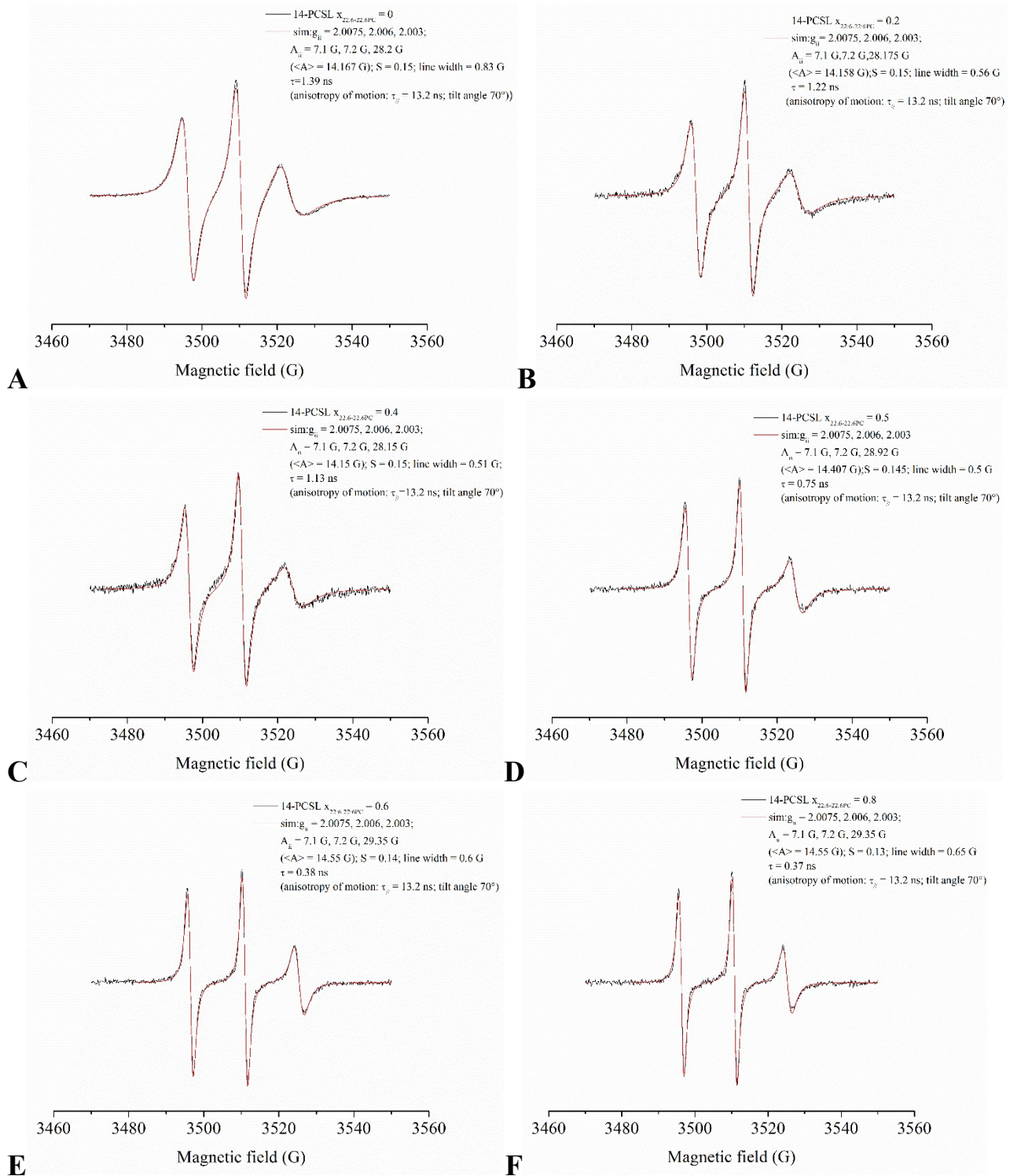


**Fig. S9** Comparison between simulated (red) and experimental (black) EPR spectra of 14-PCSL in POPC/22:6-22:6PC systems with  $x_{22:6-22:6PC}$  ranging from 0 to 0.8.